Supporting Information

A novel electrochemical sensor based on $CuFe_2O_4$/γ-CD loaded reduced graphene oxide nanocomposites: enabling the detection of metformin in water and soil

Wenwen Yi [a,b], Hua Liu [a], Yunpeng Wang [b], Jun Ma*[a], Zhongping Li*[b]

[a]*School of Environment and Resources, School of Chemical Engineering and Technology, Taiyuan University of Science and Technology, Taiyuan 030024, China*
[b] *Institute of Environmental Science and Shanxi Laboratory for Yellow River, Shanxi University, Taiyuan 030006, China.*

**Corresponding author:* Zhongping Li, Jun Ma

Email address: zl104@sxu.edu.cn, Junma0888@126.com

1. Reagents and apparatus

Ferric nitrate ($Fe(NO_3)_3$), copper nitrate ($Cu(NO_3)_2 \cdot 3H_2O$), sodium hydroxide (NaOH), potassium permanganate ($KMnO_4$), γ-Cyclodextrin ($C_{48}H_{80}O_{40}$, ⩾ 98%) were procured from Aladdin Reagent Co.,Ltd (Shanghai, China). $NaNO_3$, hydrogen peroxide (H_2O_2), Sulfuric acid (H_2SO_4, 98%), H_3PO_4 (85%), CH_3COOH (36%), H_3BO_3, Metformin ($C_4H_{11}N_5$) were supplied from Macklin Biochemical Co.,Ltd (Shanghai, China). Graphite powder was procured from Tianjin Reagent Factory. All reagents used in this research are analytically grade. Ultrapure water (18.2 MΩ) was used throughout the whole experiments. The working buffer was 0.1 M Britton-Robinson (B-R) buffer with various pH in the present study.

TEM was recorded on JEM-2100 (JEOL, Japan) for the characterization of nanomaterials. The Fourier transform infrared (FT-IR) spectra were obtained on TENSOR II infrared spectrometer (Bruker Germany). X-ray photoelectron spectroscopy (XPS) of as-prepared sample was obtained on a Thermo Scientific, ESCALAB 250Xi with Al Kα radiation (USA). UV-vis spectra were carried out on a Perkin Elmer, Lambda 950 UV-vis spectrophotometer. All electrochemical measurements were performed on a CHI760E electrochemical work-station (Shanghai Chenhua Instrument co., China) with a three-electrode system comprising a bare GCE (3 mm) or the as-prepared materials covered GCE as the working electrodes, a saturated Ag/AgCl (saturated KCl) as the reference electrode, and a Pt wires as the auxiliary electrode.

2. Synthesis of $CuFe_2O_4$/rGO

1 mmol of $Fe(NO_3)_3$ and 0.5 mmol of $Cu(NO_3)_2 \cdot 3H_2O$ were dissolved in ultrapure water (25 mL) separately and sonicated for 15 min. Subsequently, the metal salt solutions were mixed and again was sonicated for the next 15 min. Thereafter the 2 mg/mL GO solution (10 mL) was added drop by drop to the metal salt mixed solution. The mixture was adjusted to a pH of 12.0 with 6 M freshly prepared NaOH solution and sonicated again for 30 min, at room temperature, yielding a stable bottle homogeneous emulsion. Then the resulting mixture was maintained at T = 80°C, while being stirred magnetically, for 2.5 h. The black reaction dispersion was allowed to cool to room temperature, and the precipitate was centrifuged and washed with redistilled water three times. The product was finally resuspended in deionized water to obtain 1 $mg \cdot mL^{-1}$. The synthesis of $CuFe_2O_4$ is the same as the above method.

Randles equivalent circuit

R_{ct} is the charge transfer the resistance that reflects the blocking behavior of the electrode interface, C is the differential capacitance, Zw is the Warburg impedance, and Rs is Solution phase resistance.

The chemical structures of graphite, GO, and rGO were characterized using FT-IR spectroscopy (Figure S1 (A)). The graphite precursor exhibited only weak absorption peaks at 1648 cm^{-1} and 3438 cm^{-1}, attributed to the C=C vibration of its sp^2 carbon skeleton and the O-H vibration of adsorbed water, respectively. After oxidation treatment, GO showed significant characteristic peaks at 1724 cm^{-1}, 1628 cm^{-1}, 1399 cm^{-1}, and 1058 cm^{-1}, corresponding to the stretching vibrations of C=O, C=C, C-OH, and C-O bonds, respectively, along with a broad O-H absorption peak at 3395 cm^{-1}[1]. These findings collectively confirm the successful introduction of a substantial number of oxygen-containing functional groups. After reduction, the infrared absorption peaks observed for rGO at 3423 cm^{-1}, 1746 cm^{-1}, 1184 cm^{-1}, and 1400 cm^{-1} are primarily attributed to the stretching vibrations of O-H, C=O, C-O, and C-OH, respectively[2]. However, the significant decrease in intensity of peaks such as those at 1746 cm^{-1} and 1184 cm^{-1} indicates the effective removal of most oxygen-containing functional groups.

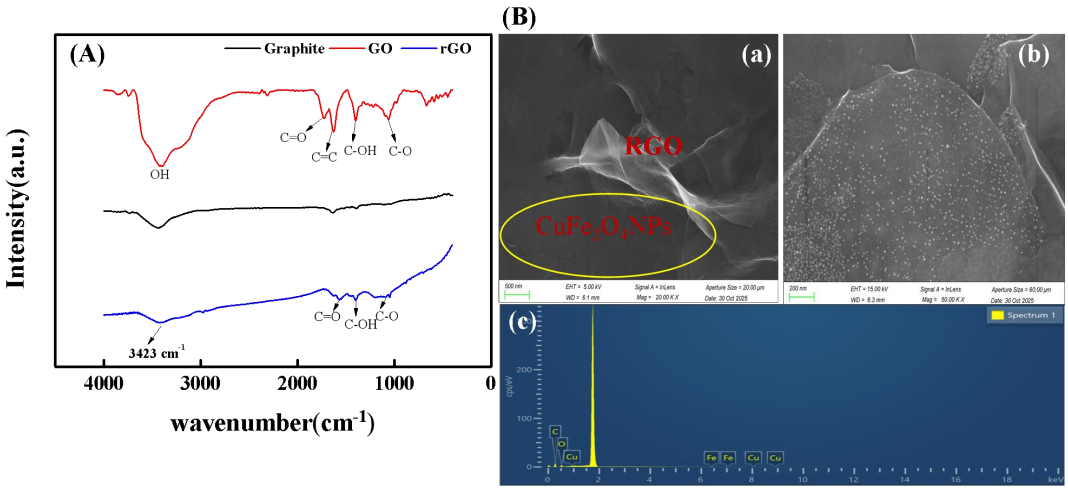

Fig. S1 (A) FT-IR spectra of graphite, GO, and rGO. (B) SEM images of $CuFe_2O_4$/rGO/γ-CD and EDS spectra.

Table. S1 C/O Ratio Analysis of $CuFe_2O_4$/rGO and $CuFe_2O_4$/rGO/γ-CD

Sample	C At%	O At%	C/O
$CuFe_2O_4$/rGO	70.15%	25.01%	2.81
$CuFe_2O_4$/rGO/γ-CD	63.90%	34.19%	1.87

Table. S2 Atomic percentage of the components of O 1s, C 1s, Fe 2p, and Cu 2p

Element	Chemical State / Assignment	$CuFe_2O_4$/rGO Atomic Percentage (At.%)	$CuFe_2O_4$/rGO/γ-CD Atomic Percentage (At.%)
C 1s	C-C	55.04%	24.78%
	C-OH	34.98%	55.58%
	-COOH	10.07%	15.05%
	C=O	-	19.64%
O 1s	Cu-O	65.14%	-
	Fe-O	34.86%	-
	Surface adsorbed -OH	56.51%	100%
Fe 2p	Fe^{2+}	39%	-
	Fe^{3+}	61%	-
Cu 2p	Cu^{2+}	51.92%	77.09%
	statellite peaks	48.08%	22.91%

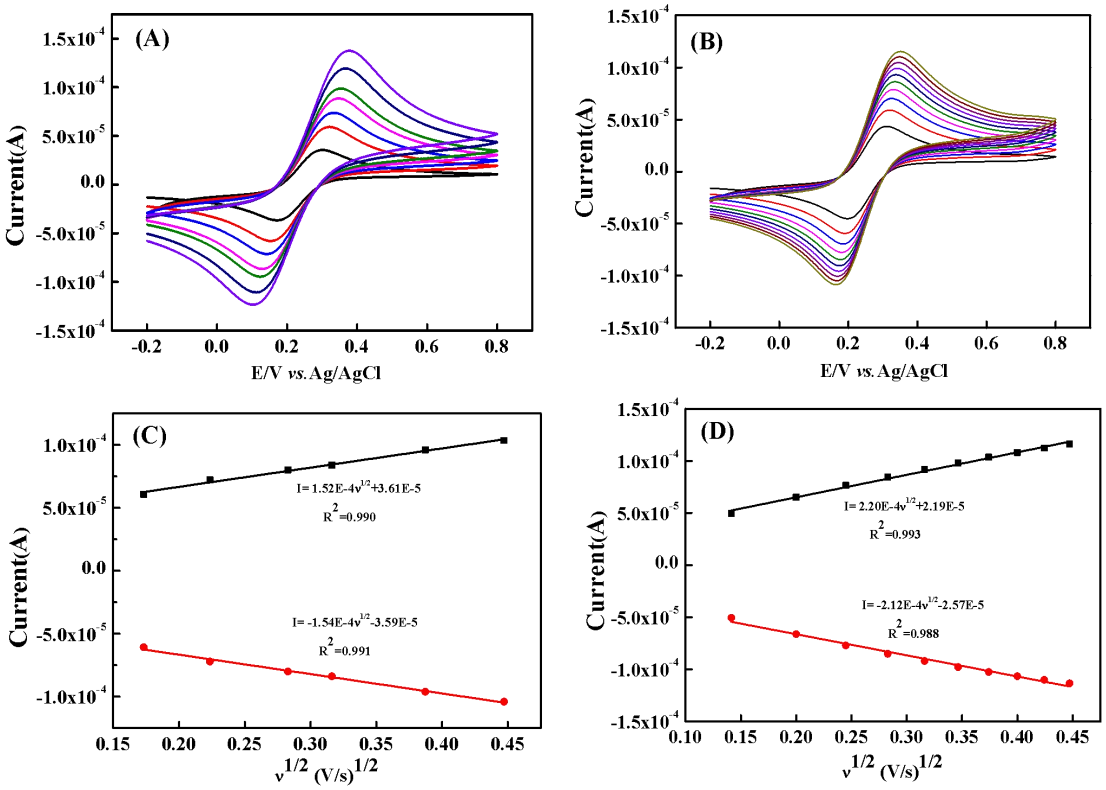

Fig. S2 CV curves of bare GCE (A) and $CuFe_2O_4$/rGO/GCE (B) with different scan rates (ν) in the presence of 5 mM $[Fe(CN)_6]^{3-/4-}$ in 0.1 M KCl solution, The inset shows the variation of the peak redox current of bare GCE (C) and $CuFe_2O_4$/rGO/GCE (D) with the $\nu^{1/2}$.

The effective electrochemical surface areas (ECSA) of different electrode materials can be calculated according to Randles-Sevcik equation[3]:

$$I=2.687*10^5 n^{3/2} A D^{1/2} C \nu^{1/2}$$

where I, n, A, D, C, and ν represent the peak current, the number of electrons (n=1), ECSA (cm^2), diffusion coefficient ($7.2*10^{-6}$ cm^2/s), solution concentration ($5*10^{-6}$ mol/cm^3) and scan rates (V/s), respectively. In this work, we used the slope of oxidation current for ECSA calculation (Fig. S2-Fig. S3). ECSA values were calculated to be 0.042 cm^2 for GCE, 0.057 cm^2 for $CuFe_2O_4$/rGO/γ-CD/GCE, 0.061cm^2 for $CuFe_2O_4$/rGO/GCE, and 0.018 cm^2 for $CuFe_2O_4$/GCE.

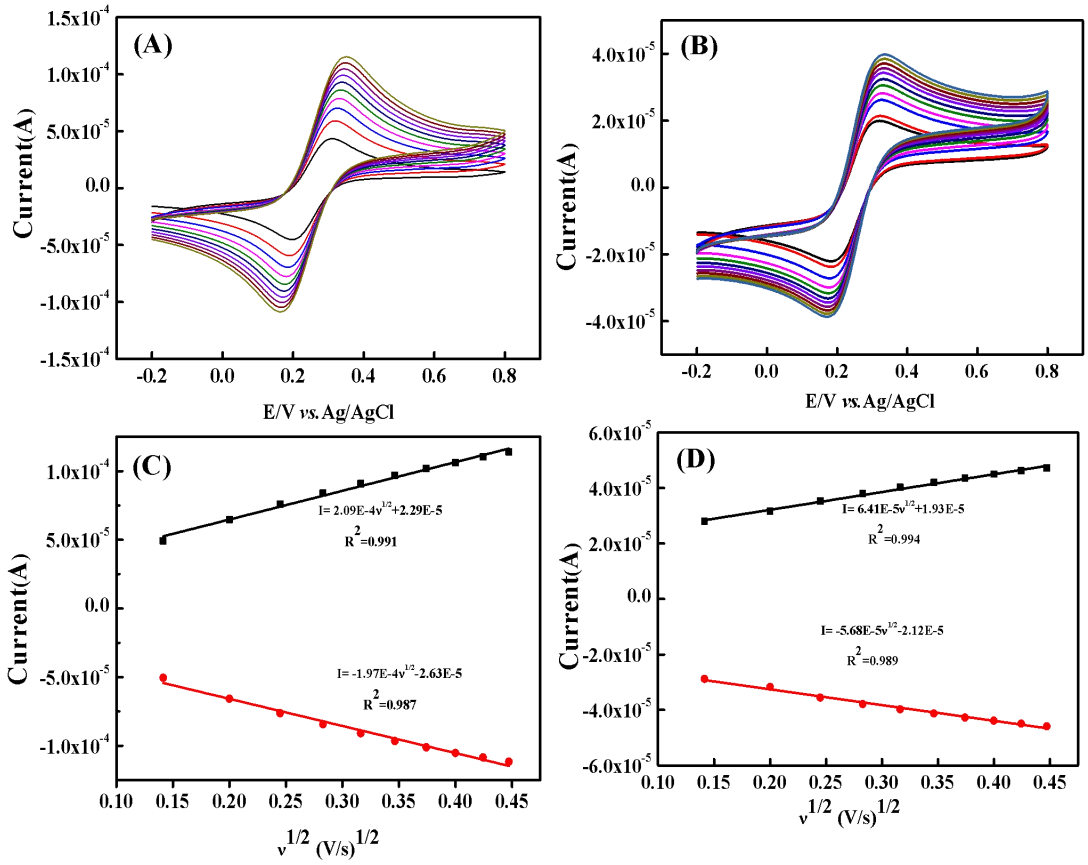

Fig. S3 CV curves of $CuFe_2O_4$/rGO/γ-CD/GCE (A) and $CuFe_2O_4$/GCE (B) with different scan rates (ν) in the presence of 5 mM $[Fe(CN)_6]^{3-/4-}$ in 0.1 M KCl solution, The inset shows the variation of the peak redox current of $CuFe_2O_4$/rGO/γ-CD/GCE (C) and $CuFe_2O_4$/GCE (D) with the $\nu^{1/2}$.

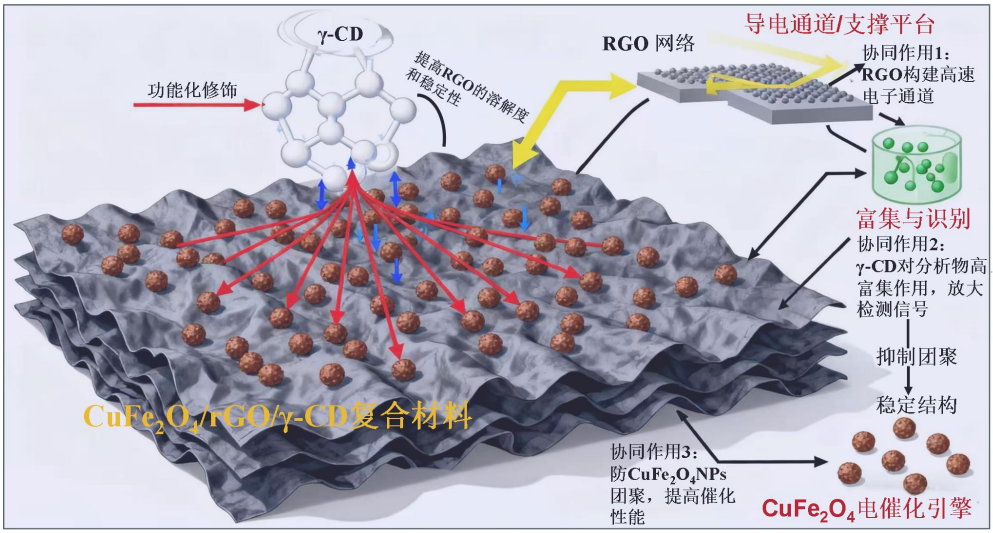

Fig. S4 Schematic diagram of the synergistic enhancement of electrochemical sensing performance by $CuFe_2O_4$/rGO/γ-CD nanocomposites

rGO, as a conductive substrate, provides a high-speed path for electron transport and prevents the agglomeration of $CuFe_2O_4$ NPs. $CuFe_2O_4$ NPs acts as a highly active catalyst, promoting the electron transfer reaction of analytes. γ-CD selectively enriches the target analyte through its cavity and "delivers" it to the vicinity of the catalytic site. The three work in synergy to jointly achieve highly sensitive and selective detection of analytes.

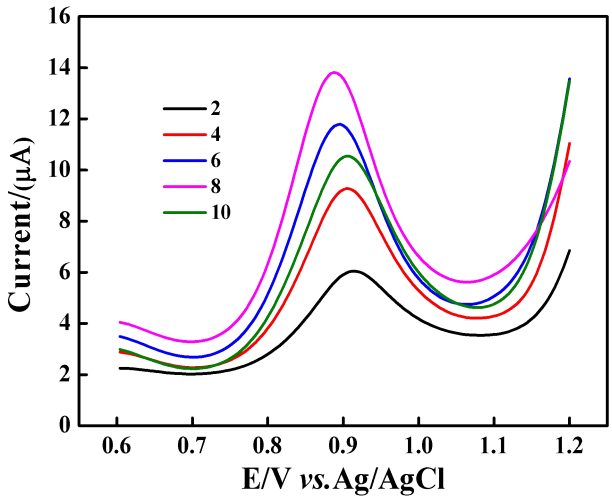

Fig. S5 The DPVs of different electrode modification amount

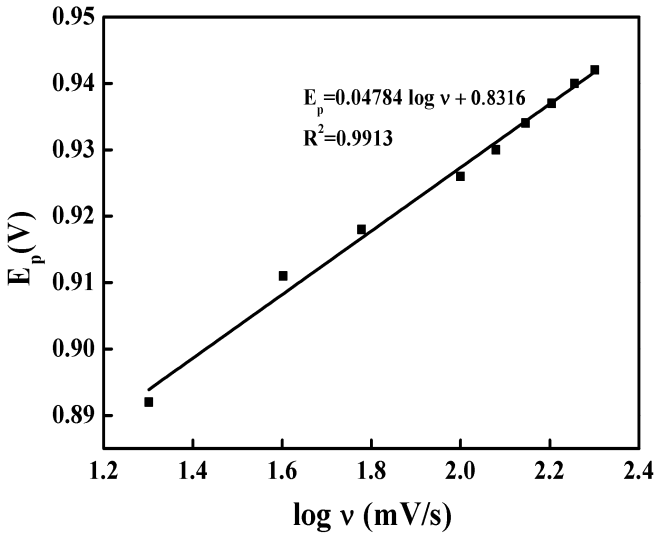

Fig. S6 Plot of the E_p versus log ν

The electron transfer number (n) and standard rate constant (k_s) of the MET oxidation process can be estimated according to Laviron's equation[4,5]:

$$E_{pa} = E^{0'} + [2.303\ RT/(1-\alpha)\ n\ F]\ \log \nu + \text{constant} \quad (1)$$

$$\log k_s = \alpha \log (1-\alpha) + (1-\alpha) \log\alpha - \log (R\ T/n\ F) - (1-\alpha)\ \alpha\ n\ F\ \Delta E_p/\ 2.3\ R\ T \quad (2)$$

Where, E_{pa} is the peak potential, $E^{0'}$ is the formal potential, R is the universal gas constant (8.314 J/mol.K), T is the absolute temperature (298.15 K), α is the electron transfer coefficient, n is electron transfer number, F is Faraday's constant 96485 C mol^{-1}), ks is standard rate constant of the reaction, ν is scan rate (V/s). From the slope of the plot in Fig.S6, the (1-α)n values are obtained as 1.23. Considering α equal to 0.50 (a value commonly assumed for organic compounds).[6,7] Thus, the values of n is estimated to be 2.46 and the n of analyte involved in the rate-determining step is 2, which is concordant with earlier studies.[8] $E^{0'}$ is obtained from the intercept of the correlation between peak potential with respect to the scan rate of the measurements (plot is not shown)[9]. The value of $E^{0'}$ obtained in this way is 0.899 V. From the intercept of the plot in Fig.S6, the value of k_s is calculated as 1.9 s^{-1}.

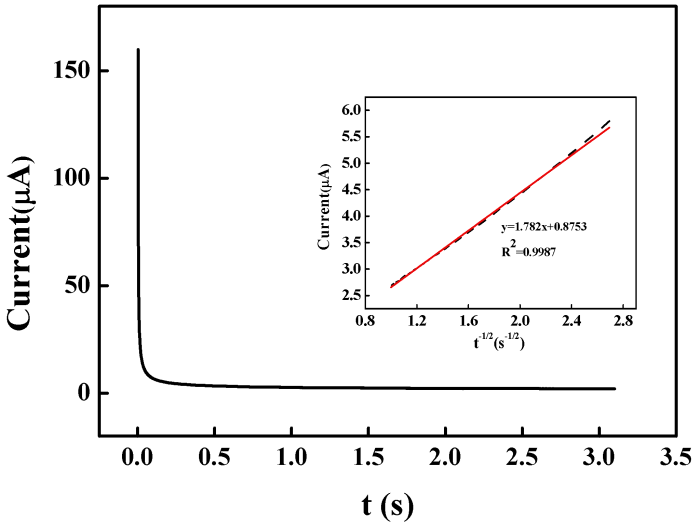

Fig. S7 The obtained chronoamperograms at $CuFe_2O_4$/rGO/γ-CD/GCE in a B-R buffer (0.1 M, pH 9) for 50 μM MET. Insets: Plots of I vs. $t^{-1/2}$ obtained from chronoamperograms.

Chronoamperometry was employed to further investigate the electrocatalytic performance of the $CuFe_2O_4$/rGO/γ-CD/GCE sensor towards MET. Figure S6 displays the chronoamperometric curves, with the inset showing the experimental plot of current (I) versus $t^{-1/2}$ along with the linear fitting result at a MET concentration of 50 μM.

Based on the Cottrell equation[10], the diffusion coefficient of MET was calculated to be 3.19×10^{-5} $cm^2 \cdot s^{-1}$. This diffusion coefficient value shows good agreement with the reported MET diffusion coefficients in the literature[11], confirming the reliability of our calculation.

$$I = nFAD^{1/2}C_b\pi^{-1/2}t^{-1/2} \qquad (3)$$

Where, n is the electron transfer number, A is the electrode area, C_b is the bulk concentration, F is the Faraday constant (96485 C/mol), and $\pi^{-1/2} \approx 0.5642$.

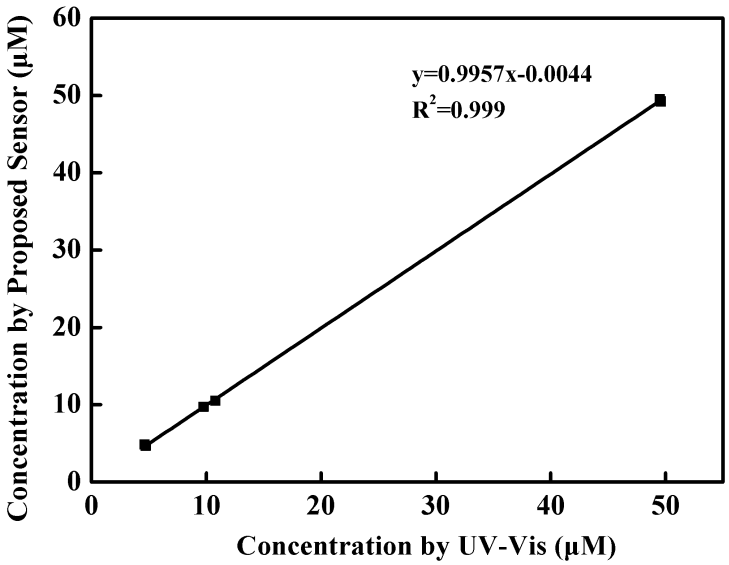

Fig. S8 Correlation between the Proposed Sensor and the Standard UV-Vis Method

Linear regression analysis of the results from all real samples (N=6) yielded a correlation equation of Y = 0.9957X - 0.0044, with a slope exceedingly close to 1 and an intercept exceedingly close to zero. This demonstrates near-perfect agreement between the proposed sensor and the standard method across the tested concentration range.

References

[1] P Lei, Y Zhou, R Q Zhu, et al. Facile synthesis of iron phthalocyanine functionalized N,B-doped reduced graphene oxide nanocomposites and sensitive electrochemical detection for glutathione. Sensor. Actuat. B-Chem., 2019, 297,126756.

[2] P Q Cao, L C Wang, Y J Xu, et al. Facile hydrothermal synthesis of mesoporous nickel oxide/reduced graphene oxide composites for high performance electrochemical supercapacitor. Electrochim. Acta, 2015, 157, 359-368.

[3] P Gao, M Z Hussain, Z Y Zhou, et al. Zr-based metalloporphyrin MOF probe for electrochemical detection of parathion-methyl. Biosens. Bioelectron., 2024, 261, 116515.

[4] A Sudarvizhi, K Pandian, O S Oluwafemi, et al. Amperometry detection of nitrite in food samples using tetrasulfonated copper phthalocyanine modified glassy carbon electrode. Sens. Actuators B Chem., 2018, 272, 151-159.

[5] O J D'Souza, R J Mascarenhas, T Thomas, et al. Platinum decorated multi-walled carbon nanotubes/Triton X-100 modified carbon paste electrode for the sensitive amperometric determination of Paracetamol. J. Electroanal. Chem., 2015, 739, 49-57.

[6] P B Deroco, R C Rocha-Filho, O Fatibello-Filho, et al. A new and simple method for the simultaneous determination of amoxicillin and nimesulide using carbon black within a dihexadecyl phosphate film as electrochemical sensor. Talanta, 2018, 179, 115-123.

[7] J J O'Dea, A Ribes, J G Osteryoung, et al. Square-wave voltammetry applied to the totally irreversible reduction of adsorbate. J. Electroanal. Chem., 1993, 345, 287-301.

[8] R Mirzajani, S. Karimi, et al. Preparation of γ-Fe_2O_3/hydroxyapatite/Cu (II) magnetic nanocomposite and its application for electrochemical detection of metformin in urine and pharmaceutical samples. Sens. Actuators B Chem., 2018, 270, 405-416.

[9] S. Sahoo, P.K. Sahoo, A. Sharma, et al. Satpati Interfacial polymerized RGO/$MnFe_2O_4$/polyaniline fibrous nanocomposite supported glassy carbon electrode for selective and ultrasensitive detection of nitrite. Sens. Actuators B Chem., 2020, 309, 127763.

[10] A J Bard, L R Faulkner, et al. Fundamentals and applications. Electrochem. Methods, second ed. Wiley, New York, 2001 (DOI).

[11] N Sattarahmadya, H Heli, F. Faramarzi, et al. Nickel oxide nanotubes-carbon microparticles/nafion nanocomposite for the electrooxidation and sensitive detection of metformin. Talanta, 2010, 82, 1126-1135.